Proc. Int. Conf. Finite Elements in Computational Mechanics, Bombay, India, 2–6 December 1985

USE OF FINITE ELEMENT TECHNIQUES TO PREDICT NONLINEAR BEHAVIOR OF REINFORCED CONCRETE STRUCTURES

W. C. Schnobrich and Hsuan-Teh Hu

Department of Civil Engineering, University of Illinois at Urbana-Champaign, USA

1. General

Reinforced concrete is by far one of the most commonly used construction materials with applications in many important categories such as tall buildings, bridges, off-shore oil platforms, nuclear containments, pressure vessels, etc. This composite material demonstrates a highly nonlinear behavior caused by cracking, aggregate interlock, bond slip, dowel action, shrinkage, creep and crushing. Because the behavior of reinforced concrete can involve many nonlinear phenomena interacting with one another, the formulation of rational analytical procedures is very difficult, and present-day design methods continue in many respects to be based on empirical approaches, using the results of a large body of experimental data assembled over many years. Such an approach has been necessary in the past, and to some extent is still necessary. However, with the help of computer, the finite element method now offers a powerful and general analytical tool for the analysis of reinforced concrete members and structures particularly some of the complex surface and shell structures that fell outside the experimental data base. The nonlinear behavior of these reinforced concrete surface and continuum structures, previously ignored or treated in a very approximate way, can now be considered rationally. Furthermore, it is possible to carry out numerical simulations of the structural response up to collapse, so that various safety aspects of the structure can be assured and its deformation characteristics can be found.

Many important classes of structures can be approximated as being in a state of plane stress. Included with this category are many of the commonly used members, such as beams, panels, slabs and thin shells. Therefore, the present paper concentrates on the biaxial states of stress for reinforced concrete.

2. Uniaxial Behavior of Concrete

Typical stress-strain curves for concrete subjected to monotonic uniaxial compression are shown in Fig. 1 (Winter and Nilson, 1979). Concrete has a nearly linear elastic behavior up to about 30 percent of its maximum compressive strength f_c'. For stress above $0.30f_c'$, microcracks form at the mortar-coarse aggregate interfaces and propagate through the mortar upon further loading (ASCE, 1981). Owning to these microcracks, concrete begins to soften until it reaches the peak stress at a strain of 0.002 to 0.003. Beyond the peak, with increasing compressive strain, damage to concrete continues to accumulate and concrete enters the decending portion of its stress-strain curve, a region marked by the appearance of macroscopic cracks.

Fig. 2 shows the stress-strain curve for concrete in uniaxial tension (Hughes and Chapman, 1966). The shape of the curve shows many similarities to the uniaxial compression. However, the maximum tensile stress is much less than the maximum compressive stress. The ratio between uniaxial tensile and compressive strength usually ranges from 0.05 to 0.1. This is not surprising since the role of microcracking must be even more important for tensional states of stress.

3. Biaxial behavior of Concrete

Under different combinations of biaxial loading, the strength and stress-strain behavior of concrete are somewhat different from those under uniaxial conditions. Fig. 3 illistrates a typical biaxial strength envelope for concrete subjected to proportional biaxial loading (Kupfer, Hilsdorf and Rusch, 1969). The maximum strength envelope seems to be largely independent of load path (Nelissen, 1972; Maekawa and Okamura, 1983). Under the condition of biaxial compression, a maximum strength increase of approimately 25 percent is achieved at a stress ratio of $\sigma_1/\sigma_2=0.5$. This increase is reduced to about 16 percent at an equal biaxial compression state ($\sigma_1/\sigma_2=1$). Under combinations of tension and compression, concrete exhibits a noticeably reduced strength. The compressive strength decreases almost linearly as the applied tensile stress is increased. Other test results (Vecchio and Collins, 1982; Maekawa and Okamura,1983) showed that principal tensile stress has a degrading effect not only on the principal compressive strength but also on the principal compressive stiffness. Under biaxial tension, concrete exhibits a nearly constant tensile strength, which is almost the same as that of its uniaxial tensile strength.

4. Failure Types and Failure Criterion for Concrete

In general, there are two types of failures for concrete, denoting these tensile and compressive types. Tensile and compressive type failures are usually characterized by brittleness and ductility, respectively. The tensile type of failure is defined as ''cracking'' where a major crack rapidly appears in the direction normal to the principal tensile stress. The compressive type of failure is defined as ''crushing'' where many small distributed cracks appear and the two principal stresses cannot be kept constant at the peak stress condition. For biaxial compression, the failure mode is the crushing type, but for biaxial tension, the failure mode is a cracking type. For tension-compression, both failure modes are observed (Maekawa and Okamura, 1983). Cracking failure will take place under stress conditions where the tensile stress is relatively large ($\sigma_1/f_t'>0.3$ and $\sigma_2/f_c'<0.85$) and crushing failure will take place under high compression-low tension stress state ($\sigma_2/f_c'>0.9$ and $\sigma_1/f_t'<0.25$). Throughout this discussion it is assumed that confinement from the third direction does not restrict movement in that direction.

There are many failure criteria proposed for concrete (Chen, 1982). Among those, the strength of concrete under combined shear and direct stress may be predicted closely by the octahedral shear stress failure criterion. This criterion relates the octahedral shear stress (τ_{oct}) to the mean stress (σ_m) at failure

$$\tau_{oct}=f(\sigma_m)$$

Mikkola and Schnobrich (1970) obtained close agreement with the experimental results of Kupfer, et al, by using linear expressions of the form

$$\tau_{oct}=a-b\,\sigma_m \tag{1}$$

where a and b are material constants. Equation (1) represents two expressions; one is valid for biaxial compression, while the other is valid for the biaxial tension and tension-compression regions. If the constants a and b are evaluated in terms of concrete strength in tension and in compression, f_t' and f_c', respectively, then Eq. (1) yields the following two expression:

$$\tau_{oct}+\sqrt{2}\,\frac{1-\alpha}{1+\alpha}\,\sigma_m-\frac{2\sqrt{2}}{3}\,\frac{\alpha}{1+\alpha}\,f'_c=0 \tag{2}$$

$$\tau_{oct}+\sqrt{2}\,\frac{\beta-1}{2\beta-1}\,\sigma_m-\frac{\sqrt{2}}{3}\,\frac{\beta}{2\beta-1}\,f'_c=0 \tag{3}$$

where α and β are given as

$$\alpha=f_t'/f_c'=0.10 \text{ and } \beta=1.16 \tag{4}$$

Equation (2) is used to indicate the boundary between cracked and uncracked concrete in biaxial tension and tension-compression regions. Equation (3) is used as a yield criterion for concrete in biaxial compression. These equations have a discontinuity at points $(0,f_c')$ and $(f_c',0)$, where either equation could be used. Yielded concrete will crush under further loading. Hand, Pecknold and Schnobrich (1972) have used a strain-based criterion to determine the crushing boundary. It is accomplished by replaceing f_c' with the concrete crushing strain ε_u, τ_{oct} with the octahedral shearing strain ε_{oct}, and σ_m with the mean strain ε_m in equation (3). The criterion is given as follows

$$\epsilon_{oct}+\sqrt{2}\,\frac{\beta-1}{2\beta-1}\,\epsilon_m-\frac{\sqrt{2}}{3}\,\frac{\beta}{2\beta-1}\,\epsilon_u=0 \tag{5}$$

where

$$\epsilon_m = \frac{1}{3}(\epsilon_{xx} + \epsilon_{yy} + \epsilon_{zz})$$

$$\epsilon_{oct} = \frac{1}{3}\left[(\epsilon_{xx} - \epsilon_{yy})^2 + (\epsilon_{yy} - \epsilon_{zz})^2 + (\epsilon_{zz} - \epsilon_{xx})^2 + 6(\epsilon_{xy}^2 + \epsilon_{yz}^2 + \epsilon_{zx}^2)\right]^{\frac{1}{2}}$$

5. Plasticity-Based Model for Concrete

When concrete is subjected to compressive stresses, experimental results (Sinha, Gerstle and Tulin, 1964) have indicated that the nonlinear deformations of concrete are basically inelastic, because upon unloading only a portion of the strains can be recovered from the total strains (Fig. 4). Therefore, the stress-strain behavior may be separated into the recoverable part which can be treated within elasticity theory and the irrecoverable parts which can be treated by plasticity theory. Plasticity based models have been extensively used in recent years to describe the behavior of concrete. Initial plasticity models described concrete as an elastic-perfectly plastic material (Mikkola and Schnobrich, 1970; Hand, Pecknold and Schnobrich, 1972; Abdel Rahman, 1982). Later models incorporated a hardening behavior (Chen and Chen, 1975; Buyukozturk, 1977; Chen and Ting, 1980).

6. Elastic-Perfectly Plastic Model

Under high compression, it is know that concrete undergoes flow somewhat like a ductile material on the yield surface before reaching its crushing surface (analogous to the yield surface but in terms of strain). This limited plastic flow ability of concrete before crushing can be represented by the introduction of a elastic-perfectly plastic model.

6.1 Criterion of Loading and Unloading

For an elastic-perfectly plastic material, the general behavior under a complex stress state can be defined by the following three statements:

1. The material is elastic until it reaches the yield limit. This is known as the yield function

$$f(\{\sigma\}) = K \tag{6}$$

where K is a material constant and $\{\sigma\} = |\sigma_{xx}, \sigma_{yy}, \tau_{xy}|^T$ are the inplane stress components.

2. Then plastic deformation takes place up to the crushing surface. For the plastic flow to continue, the state of stress must remain on the yield surface. Thus the loading criterion is

$$df = \frac{\partial f}{\partial \{\sigma\}} d\{\sigma\} = 0 \tag{7}$$

3. When the stress intensity drops below the yield value, the flow strain is permanent and the unloading criterion is

$$df = \frac{\partial f}{\partial \{\sigma\}} d\{\sigma\} < 0 \tag{8}$$

In general, the yield function $f(\{\sigma\}) = K$ represents a hypersurface in a three-dimensional stress space. Fig. 5 shows those three states and yield surface in a two dimensional principal stress space.

6.2 Flow Rule and Normality Law

The total strain experienced by a plastic body is the sum of the elastic and plastic strains, $\{\varepsilon\}_e$ and $\{\varepsilon\}_p$. That is

$$\{\epsilon\} = \{\epsilon\}_e + \{\epsilon\}_p \tag{9}$$

where $\{\epsilon\} = |\epsilon_{xx}, \epsilon_{yy}, \gamma_{xy}|^T$. If in terms of incremental strains

$$d\{\epsilon\} = d\{\epsilon\}_e + d\{\epsilon\}_p \tag{10}$$

When the material deforms plastically, we can relate the plastic incremental strains $d\{\varepsilon\}_p$ with a plastic potential function $g(\{\sigma\})$ by the following equation

$$d\{\epsilon\}_p = d\lambda \frac{\partial g}{\partial \{\sigma\}} \tag{11}$$

where $d\lambda$ is a positive scalar factor. In the simplest case when the yield function and plastic potential function coincide f = g. Then,

$$d\{\epsilon\}_p = d\lambda \frac{\partial f}{\partial \{\sigma\}} \tag{12}$$

Equation (12) is called the associated flow rule because it is connected with the yield criterion. If $f \neq g$, equation (11) is called the nonassociated flow rule. The associated flow rule has been used by a lot of investigators (Mikkola and Schnobrich, 1970; Hand, Pecknold and Schnobrich, 1972; Abdel Rahman, 1982). But the need for a nonassociated flow rule has been demonstrated by numerical results of some practical problems (Vermeer and Borst, 1984). For convenience, let

$$\{a\}^T = \frac{\partial f}{\partial \{\sigma\}} = \left[\frac{\partial f}{\partial \sigma_{xx}}, \frac{\partial f}{\partial \sigma_{yy}}, \frac{\partial f}{\partial \tau_{xy}}\right] \tag{13}$$

$$\{b\}^T = \frac{\partial g}{\partial \{\sigma\}} = \left[\frac{\partial g}{\partial \sigma_{xx}}, \frac{\partial g}{\partial \sigma_{yy}}, \frac{\partial g}{\partial \tau_{xy}}\right] \tag{14}$$

where {a} and {b} are the flow vectors associated with potential functions f and g. From equation (7), when plastic deformation takes place, we have

$$df = \frac{\partial f}{\partial \{\sigma\}} d\{\sigma\} = \{a\}^T d\{\sigma\} = 0$$

Multiplying the equation by dλ the following expression is obtain

$$d\lambda \{a\}^T d\{\sigma\} = d\{\epsilon\}_p^T d\{\sigma\} = 0 \tag{15}$$

Since d{σ} is tangential to yield surface, with the associated flow rule (12), the incremential plastic strain must be normal to the yield surface. Equation (15) is called the normality law. It should be noted that if a nonassociated flow rule is used, the incremental plastic strains are no longer normal to the yield surface.

6.3 Incremental Stress-Strain Relationships

The elastic or recoverable strain increments $d\{\varepsilon\}_e$, can be assumed to be given by a generalized Hooke's law. In abbreviated form

$$d\{\sigma\} = |\ C\ |_e\ d\{\epsilon\}_e \tag{16}$$

where $[C]_e$ is the elastic stiffness matrix and is given as follows

$$|\ C\ |_e = \frac{E_c}{1-\mu^2} \begin{bmatrix} 1 & \mu & 0 \\ \mu & 1 & 0 \\ 0 & 0 & \frac{1-\mu}{2} \end{bmatrix} \tag{17}$$

In this equation E_c is the Young's modulus of concrete and μ is the Poisson's ratio. Now substitution of equation (10) into equation (16) yields

$$d\{\sigma\} = |C|_e (\ d\{\epsilon\} - d\{\epsilon\}_p) \tag{18}$$

Considering the general flow rule, the incremental form of the stress-strain relation, written in terms of total strain is

$$d\{\sigma\} = |\ C\ |_{ep}\ d\{\epsilon\} \tag{19}$$

where

$$|\ C\ |_{ep} = |\ C\ |_e + |\ C\ |_p$$

and

$$|C|_p = -\frac{|C|_e \{b\}\{a\}^T |C|_e}{\{a\}^T |C|_e \{b\}} \tag{20}$$

Since $[C]_e$ is symmetric, $[C]_{ep}$ will also be symmetric, if associated flow rule is used (ie, f ≡ g). Otherwise, $[C]_{ep}$ is unsymmetric. It should be noted that the matrix $[C]_{ep}$ is singular.

7. Elastic-Strain Hardening Plastic Model

A generalization of the elastic-perfectly plastic model can be made by the use of the strain-hardening theory of plasticity in establishing the constitutive relations for concrete. The primary characteristics of this model is the introduction of the pressure sensitivity of inelastic behavior. With this approach an initial yield surface is defined as the limiting surface for elastic behavior and this surface is located at a certain distance from the failure surface. Fig. 6 shows the projections of these two limiting surfaces in a two dimensional principal stress space. When the state of stress lies within the initial yield surface, the material behavior is assumed to be in the elastic range. When the material is stressed beyond the elastic limit surface, a subsequent new discontinuity surface is developed and replaces the initial yield surface. Unloading and reloading of the material within this subsequent loading surface results in elastic behavior, and no additional plastic deformation will occur until this new surface is reached. Further discontinuity surface and additional plastic deformations will result, if loading is continued beyond this surface. Final collapse of the concrete is defined when the failure surface is reached and concrete cracking or crushing occurs.

7.1 Hardening Rule

The hardening rule defines the motion of the subsequent yield surface during plastic loading. A number of hardening rules have been proposed, such as isotropic hardening, kinematic hardening and mixed hardening rules. For the monotonic loading case, because no reverse loading takes place it is convenient to use the isotropic hardening rule to simulate the concrete behavior. An isotropic hardening rule assumes that the yield surface expands uniformly without distortion as plastic flow occurs (Fig. 7). This hardening rule implies that because of hardening the material will exhibit an increase in the compressive yield stress equal to the increase in the tensile yield stress.

7.2 Criterion of Loading and Unloading

For elastic-strain hardening concrete, a yield function can be defined by the relation

$$f(\ \{\sigma\}, K\ ) = F(\ \{\sigma\}\ ) - K \tag{21}$$

such that whenever the function F becomes equal to the value of K yielding would begin and K takes on a new value. The function F can then be looked upon as a loading function and K is a yield function which depends on the complete previous stress and strain history of the material and its strain-hardening properties. We can now distinguish four cases for a strain-hardening model:

1. $f = 0,\ dF = \frac{\partial F}{\partial \{\sigma\}} d\{\sigma\} > 0$ (22)

   f = 0 means the stress state is on the yield surface. dF > 0 means the stress state is moving out from the yield surface and plastic flow is occuring. This constitutes loading.

2. $f = 0,\ dF = \frac{\partial F}{\partial \{\sigma\}}\, d\{\sigma\} = 0$ (23)

dF = 0 correspponds to the case of the stress state moving on the yield surface and is called neutral loading. No plastic flow will occur.

3. $f = 0,\ dF = \frac{\partial F}{\partial \{\sigma\}}\, d\{\sigma\} < 0$ (24)

dF < 0 means the stress state is moving in from the yield surface and unloading is taking place.

4. If $f < 0$, the stress state is an elastic one.

7.3 Effective Stress and Effective Plastic Strain

In the strain-hardening theory of plasticity, the hardening parameters in the loading function can be related to the experimental uniaxial stress-strain curve. In this way, some stress variable called effective stress and some strain variable called effective plastic strain are needed, so they can be plotted against each other and used to correlate the test results.

Because the loading function F({σ}) determines whether additional plastic flow takes place or not and is also a positively increasing function, it can be used as a stress variable to define the effective stress as follows

$$F(\{\sigma\}) = CS^n \tag{25}$$

Where S is the effective stress and C and n are constants dependent on the loading function. To determine the effective plastic strain ϵ_p, the general way is to define the effective plastic strain increment as some combination of plastic strain increments. The simplest type is

$$d\epsilon_p = d\lambda = D\sqrt{\{\epsilon\}_p^T\, d\{\epsilon\}_p} \tag{26}$$

where D is a constant.

The effective stress-effective plastic strain relation has the general form

$$S = S(\epsilon_p) \tag{27}$$

Differentiating equation (27) yields

$$dS = h(S)\, d\epsilon_p \tag{28}$$

where h is the slope of the effective stress-effective plastic strain curve at the current value of S. The intergrated effective plastic strain is a function of effective stress only.

$$\epsilon_p = \int \frac{dS}{h(S)} \tag{29}$$

7.4 Incremental Stress-Strain Relationships

Once the loading surface is defined, incremental plastic stress-strain relations based on the flow rule are applicable to such a material model and the corresponding constitutive equations can then be derived. Recall equation (18)

$$d\{\sigma\} = [C]_e\,(\,d\{\epsilon\} - d\{\epsilon\}_p\,) \tag{18}$$

Recall flow rule (11), flow vectors (13) and (14). Then, multiply the above equation by $\{a\}^T$

$$\{a\}^T d\{\sigma\} = \{a\}^T [C]_e\,(\,d\{\epsilon\} - d\lambda\{b\}\,) \tag{30}$$

However,

$$\{a\}^T\, d\{\sigma\} = dS = h\, d\epsilon_p = h\, d\lambda \tag{31}$$

Substitute equation (31) into equation (30) and solve for dλ

$$d\lambda = \frac{\{a\}^T [C]_e\, d\{\epsilon\}}{h + \{a\}^T [C]_e \{b\}} \tag{32}$$

Rewrite equation (18). Then

$$d\{\sigma\} = [C]_e(\,d\{\epsilon\} - d\lambda\{b\}\,) \tag{33}$$

Substituting equation (32) into equation (33) yields

$$d\{\sigma\} = [C]_{ep}\, d\{\epsilon\} \tag{34}$$

where

$$[C]_{ep} = [C]_e + [C]_p$$

and

$$[C]_p = -\frac{[C]_e\{b\}\{a\}^T [C]_e}{h + \{a\}^T [C]_e \{b\}} \tag{35}$$

If the associated flow rule is used (ie. f = g), $[C]_{ep}$ will be symmetric. Otherwise, $[C]_{ep}$ is unsymmetric. It should be noted that when the hardening parameter h = 0, equation (35) reduces to equation (20), which is the incremental stress-strain relationships for elastic-perfectly plastic model.

8. Concrete Cracking

There are two competing criteria for determining the initiation and propagation of cracking in concrete, a strength criterion and one based on fracture mechanics concepts. With a strength criterion, in tension dominated regions, tensile cracks occur as soon as the tensile strength of plain concrete is exceeded in the cracking direction or alternatively when the maximum tensile strain is attained in some direction. With the

fracture mechanics approach, propagation hinges on the level of the fracture energy. In the finite-element analysis of concrete, two different approaches have been employed to model concrete cracking: the discrete and the smeared crack representations. Both of these resprentations have been employed using both the strength criterion and the fracture mechanics approach. The smeared crack concept is more in keeping with the philosophy of the finite element method with its continuous displacement.

In the discrete crack system, a crack is modeled by disconnecting or separating elements on each side of a node thereby the splitting the node and requiring additional nodes (Ngo and Scordelis, 1967; Nilson, 1968). This procedure therefore actually produces a crack by the physical separation into two sides across a crack, as shown in Fig. 8. However, difficulties encountered in the redefining of the finite element topology and the lack of generality in possible crack directions have restricted the use of discrete crack models. The most successful use of discrete cracking has been with fracture mechanics (Saouma and Ingraffea, 1981). However the computational activity for such approaches especially when they regrid during the solution process makes them impractical for any but special research problems.

In the smeared crack system, introduced by Rashid (1968), cracked concrete is assumed to remain a continnum. A crack is not discrete but implies an infinite number of parallel fissures across that part of the finite element (Fig. 9). After cracking has occurred, the cracked concrete becomes an orthotropic material. The incremental stress-strain relationships associated with the coordinate system alined to the cracked direction become

$$\begin{Bmatrix} d\sigma_1 \\ d\sigma_2 \\ d\tau_{12} \end{Bmatrix} = \begin{bmatrix} 0 & 0 & 0 \\ 0 & E_c & 0 \\ 0 & 0 & \beta G \end{bmatrix} \begin{Bmatrix} d\epsilon_1 \\ d\epsilon_2 \\ d\gamma_{12} \end{Bmatrix} \tag{36}$$

With early smeared crack models, the modulus of elasticity of concrete is reduced to zero in the direction normal to the crack axis. Further, a reduced shear stiffness βG is assumed on the cracked plane to account for the aggregate interlocking or shear friction that are presented at the crack surface. The pratical value chosen for β (between 0 and 1) does not appear to be critical for problems on which a simple strength criterion is a reasonable strategy for crack definition (Hand, Pecknold and Schnobrich, 1972; Lin and Scordelis, 1975; ASCE, 1981), but values greater than zero are necessary to prevent numerical difficulties. On the other hand problems in which a dominant crack developes and the more elaborate fracture mechanics approach must be formulated, the β function becomes much more sensitive (Rots, et. al., 1985). Several questions have been raised regarding the validity of the smeared crack process based on a strength criterion (Bazant and Cedolin, 1979). These questions focus on the objectivity of the crack process if strength controlled and on the development of strain localization. Strain localization can be accompanied by numerical instability problems which are partially stabilized when reinforcing is included (Rots, 1985).

In most crack models, the crack direction is assumed fixed once it forms and while it remains open. Several references restrict secondary cracking to form orthogonal to the primary crack (Darwin and Pecknold, 1974; Kabir, 1976). However, analytical models which incroporate a shear

retention factor βG should allow rotation of the concrete principal stress directions after initial cracking, and the second crack need not be perpendicular to the first crack. This restriction may violate the cracking criterion within the element, therefore, a nonorthogonal crack model is more realistic (Abdel Rahman, 1982). After two cracks take place, the incremental stress-strain relationships become

$$\begin{Bmatrix} d\sigma_1 \\ d\sigma_2 \\ d\tau_{12} \end{Bmatrix} = \begin{bmatrix} 0 & 0 & 0 \\ 0 & 0 & 0 \\ 0 & 0 & \beta G \end{bmatrix} \begin{Bmatrix} d\epsilon_1 \\ d\epsilon_2 \\ d\gamma_{12} \end{Bmatrix} \tag{37}$$

A consistent shear retention model for nonorthogonal cracks can be developed by requiring equal shear stresses on the nonorthogonal crack faces. In doing so it is convenient to orient the orthogonal reference axis with one axis bisecting the nonorthogonal crack directions (ASCE, 1981; Abdel Rahman, 1982). When such a shear retention model is used, a third crack can form and the cracked concrete will lose all the stiffness.

The other kind of cracking model is the rotation crack model. Experiments by Vecchio and Collins (1982) indicate that the ''average crack direction'' does change as the loading increases, as initially formed cracks become less prominent and new cracks are formed. This average crack direction is defined to be perpendicular to the maximum principal strain. Gupta and Habibollah (1982) have developed an alogorithm which allows for the changing crack direction effect and this algorithm has been implemented by Milford and Schnobrich (1984).

9. Tension Stiffening

As the concrete reaches its tensile strength, primary cracks form. At the primary cracks, the concrete stress drops to zero and steel carries the full load. However, between the cracks the load is shared between steel and concrete (Fig. 10). This ability of concrete between cracks to carry some tensile load and to contribute to the overall stiffness of the system is called ''tension stiffening'' . The tension stiffening effect has been represented in two ways. In one case, the tension portion of the concrete stress-strain curve has been given a descending branch (Lin and Scordelis, 1975) as shown in Fig. 11. The second method is to increase the steel stiffness (Gilbert and Warner, 1978) as shown in Fig. 12. The additional stress in the steel represents the total tensile force carried by both the steel and the concerte between the cracks. The added stress is lumped at the level of the steel and oriented in the same direction for reasons of convenience.

10. Some Applications

With the employment of nonlinear finite element analysis of reinforced concrete structures the structural engineer can establish load capacities and structural behavior of a number of structures. For many structures such an analysis is unnecessary. Capacities and behavior can be much more easily and economically established. For some classes of structures however this is not the case, for example surface and shell structures. Here the element method does provide the engineer with insights into how such structures soften and fail, insights that he could

not acquire by other means.

Several investigations into failure loads for shell type structures have taken the form of strength based cracking finite element models with both elasticity and hardening models. These models are subject to the questions of the correctness of the strength based model, the problems of objectivity and localizations. With shell structures the problems are compounded because of the sensitivity of the results to the chosen shell element. Shear and membrane locking of many elements can induce significantly more of this type of stress than should prevail. Futhermore the positioning of the stress points, particularly with numerically integrated elements, moves the stress monitoring point away from the region of peak values. These factors coupled with the computational intensity of these problems results in element meshes of sufficient dimension that the question of objectivity of strength based cracking process does not appear to be a dominant factor.

To illustrate the type of answers and insights that can be gained two shells are discussed. For the first shell a hypar studied by Chan (1982) is presented. This shell is in a gable roof configuration. The mesh of 9 node Lagrangian shell elements used by Chan is shown in Fig. 13. The Darwin (1974) model was used to define the concrete properties with a strength based cracking model which included tension stiffening within the steel properties. This investigations also included creep a particularly and nonlinear geometry effects. Significant result that Chan observed was a marked reduction in failure load as a consequence of creep, Fig. 14. The failure mechanism seems to involve the influence of creep on the support the shell provides the ridge beam. The consequence of the reduction in support translates into increased moments and a significant shift on the interaction diagram.

The second shell problem discussed is the wind load on a cooling tower (Milford and Schnobrich, 1984). The shell is also modeled by 9 node Lagrangian shell elements Fig. 15. This study also used a strength criterion on cracking but with tension stiffening. Loading was wind Because the steel percentages in the circumferential and meridional directions are markedly different the cracking model included a rotating crack capability. Of particular note in this study is the dependence of the result on the selected tension stiffening Fig. 16. The shell demonstrated an inability to redistribute circumferentially around the shell due to the constraints placed by the wind load distribution. Thus a fully developed ultimate load for a beam whose cross section is composed of an open circular section with an enclosed angle of approximately 135° was not able to develop.

These studies demonstrate the class of problems that the nonlinear analyses can address and that significant engineering results can be achieved using basic concrete material models for surface and shell structures.

11. References

1. Abdel Rahman, H. H., ''Computational Models for the Nonlinear Analysis of Reinforced Concrete Flexural Slab System'', Ph.D. Thesis, University College of Swansea, 1982.

2. ASCE Task Committee on Concrete and Masonary Structure, ''State of the Art Report on Finite Element Analysis of Reinforced Concrete'', ASCE, 1981.

3. Bazant, Z. P., ''Advances in Deformation and Failure Modes for Concrete'', Introductory Report, IABSE Colloquium on Advanced Mechanics of Reinforced Concrete, Delft, June 1981, pp. 9-39.

4. Bazant, Z. P. and Cedolin, L., ''Blunt Crack Band Propagation in Finite Element Analysis'', Journal of the Engineering Mechanics Division, ASCE, Vol. 105, No. EM2, 1979, pp. 297-315.

5. Buyukozturk, O., ''Nonlinear Analysis of Reinforced Concrete Structure'', Computers and Structures, Vol. 7, 1977, pp. 149-156.

6. Chan, E. C., ''Nonlinear Geometric Material and Time Dependent Analysis of Reinforced Concrete Shells with Edge Beams'', University of Calinfornia Berkeley Report SESM-82/08, 1982.

7. Chen, A. C. T., and Chen, W. F., ''Constitutive Relations for Concrete'', Journal of the Engineering Mechanics Division, ASCE, Vol. 101, No. EM4, Proc. Paper 11529, August, 1975, pp. 465-481.

8. Chen, W. F., ''Plasticity in Reinforced Concrete'', McGraw-Hill, New York, 1982.

9. Chen, W. F. and Ting, E. C., ''Constitutive Models for Concrete Structures'', Journal of the Engineering Mechanics Division, ASCE, Vol. 106, No. EM1, Proc. Paper 15177, February 1980, pp. 1-19.

10. Darwin, D. and Pecknold, D. A., ''Inelastic Model for Cyclic Biaxial Loading for Reinforced Concrete'', Civil Engineering Studies, SRS No. 409, University of Illinois, Urbana, Illinois, July 1974.

11. Gerstle, K. H., ''Material Modelling of Reinforced Concrete'', Introductory Report, IABSE Colloquium on Advanced Mechanics of Reinforced Concrete, Delft, June 1981, pp. 41-61.

12. Gibert, R. I. and Warner, R. F., ''Tension Stiffening in Reinforced Concrete Slabs'', Journal of the Structural Division, ASCE, Vol. 104, No. ST12, Proc. Paper 14211, December 1978, pp. 1885-1900.

13. Gupta, A. K., ''Membrane Reinforcement in Shells'', Journal of the Structural Division, ASCE, Vol. 107, No. ST1, Proc. Paper 15975, January 1981, pp. 41-56

14. Gupta, A. K. and Habibollah, A., ''Changing Crack Direction in Reinforced Concrete Analysis'', Report, Civil Engineering Department, North Carolina State University, Raleigh, North Carolina, January 1982.

15. Hand, F. R., Pecknold, D. A. and Schnobrich, W. C., ''A Layered Finite Element Nonlinear Analysis of Reinforced Concrete Plates and Shells'', Civil Engineering Studies, SRS No. 389, University of Illinois, Urbana, Illinois, August 1972.

16. Hughes, B. P. and Chapman, C. P., ''The Deformation of Concrete and

Microconcrete in Compression and Tension with Particular Reference to Aggregate Size'', Magazine of Concrete Research, Vol. 18, No. 54, Great Britain, March 1966, pp. 19-24.

17. Jan, Wastiels, ''A Softening Plasticity Model for Concrete'', Numerical Methods for Nonlinear Problem, Part I, Proc. of the Int. Conf. held at the University College of Swansea (U. K.), Pineridge Press, Swansea, September 1980, pp. 481-492.

18. Kabir, A. F., ''Nonlinear Analysis of Reinforced Concrete Panels, Slabs and Shell for Time Dependent Effects'', Ph.D. Thesis, UC-SESM 76-6, University of California, December 1976.

19. Kupfer, H. B., Hilsdorf, H. K. and Rusch, H., ''Behavior of Concrete Under Biaxial Stresses'', Journal of the American Concrete Institute, Vol. 66, No. 8, August 1969, pp. 656-666.

20. Lin, C. S. and Scordelis, A., ''Nonlinear Analysis of RC Shells of General Form'', Journal of the Structural Division, ASCE, Vol. 101, No. ST3, Proc. Paper 11164, March 1975, pp. 523-538.

21. Maekawa, K. and Okamura, H., ''The Deformational Behavior and Constitutive Equation of Concrete Using the Elasto-Plastic and Fracture Model'', Journal of the Faculty of Engineering, The University of Tokyo, Vol. XXXVII, No. 2, 1983, pp. 253-328.

22. Mikkola, M. J. and Schnobrich, W. C., ''Material Behavior Characteristics for Reinforced Concrete Shell Stressed Beyond the Elastic Range'', Civil Engineering Studies, SRS No. 367, University of Illinois, Urbana, Illinois, August 1970.

23. Milford, R. V. and Schnobrich, W. C., ''Nonlinear Behavior of Reinforced Concrete Cooling Towers'', Civil Engineering Studies, SRS No. 514, University of Illinois, Urbana, Illinois, May 1984.

24. Nelissen, L. J. M., ''Biaxial Testing of Normal Concrete'', Heron, Delft, the Netherlands, Vol. 18, No. 1, 1972.

25. Ngo, D., and Scordelis, A.C., ''Finite Element Analysis of Reinforced Concrete Beams'', Journal of the American Concrete Institute, Vol. 64, No. 3, March 1967, pp. 152-163.

26. Nilson, A. H., ''Nonlinear Analysis of Reinforced Concrete by the Finite Element Method'', Journal of the American Concrete Institute, Vol. 65, No. 9, September 1968, pp. 757-766.

27. Ottosen, N. S., ''Constitutive Model for Short-Time Loading of Concrete'', Journal of the Engineering Mechanics Division, ASCE, Vol. 105, No. EM1, Proc. Paper 14375, February 1979, pp. 127-141.

28. Rashid, Y. R., ''Analysis of Prestresses Concrete Pressure Vessels''. Nuclear Engineering and Design, Vol. 7, No. 4, April 1968, pp. 334-344.

29. Rots, J. G., Nauta, P., Kusters, J. B., ''Smeared Crack Approach and Fracture Localization in Concrete'', Heron, Delft, the Netherlands, Vol. 30, No. 1, 1985.

30. Saouma, V. E. and Ingraffea, A. R., ''Fracture Mechanics Analysis of Discrete Cracking'', Final Report, IABSE Colloquium on Advanced Mechanics of Reinforced Concrete, Delft, June 1981, pp. 413-436.

31. Schnobrich, W. C., ''Behavior of Reinforced Concrete Structures Predicted by the Finite Element Method'', Computers and Structures, Vol. 7, June 1977, pp. 365-376.

32. Sinha, B. P., Gerstle, K. H. and Tulin, L. G., ''Stress-Strain Relations for Concrete Under Cyclic Loading'', Journal of the American Concrete Institute, Vol. 61, No. 2, February 1964, pp. 195-211.

33. Vecchio, F. and Collins, M. P., ''The Response of Reinforced Concrete to Inplane Shear and Normal Stresses'', Publication No. 82-03, University of Toronto, March 1982.

34. Vermeer, P. A. and Borst, R. DE, ''Non-associated Plasticity for Soils, Concrete and Rock'', Heron, Delft, the Netherlands, Vol. 29, No. 3, 1984, pp. 5-64.

35. Winter, G. and Nilson, A. H., ''Design of Concrete Structures'', 9th Edition, McGraw-Hill, New York, 1979, pp. 16.

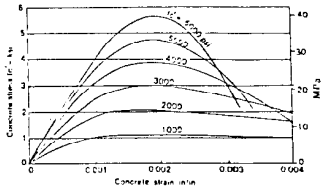

Fig. 1 Typical Stress-Strain Curves of Concrete in Compression.
(Winter and Nilson, 1979)

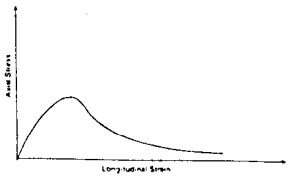

Fig. 2 Stress-Strain Curve of Concrete in Tension.
(Nagaoka and Okamura, 1984)

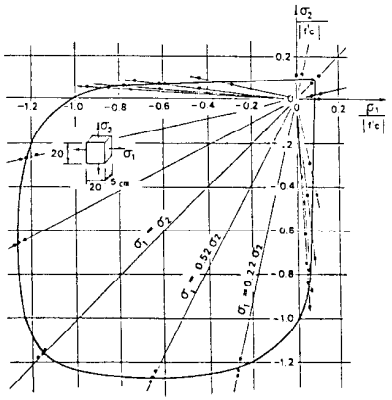

Fig. 3 Biaxial Strength of Concrete.
(Kupfer, Hilsdorf and Rusch, 1969)

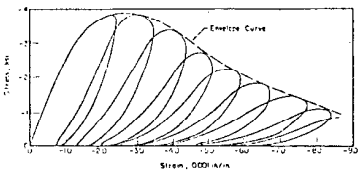

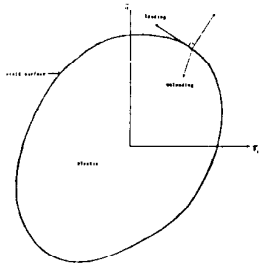

Fig. 5 Yield Surface and Subsequent of Loading and Unloading

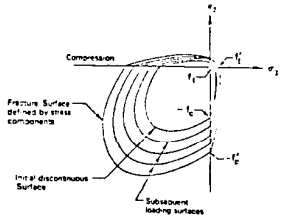

Fig. 6 Loading surfaces of Concrete in the Biaxial Stress Plane

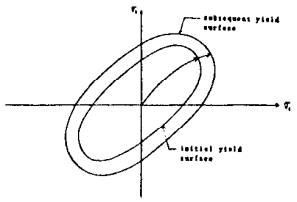

Fig. 7 Subsequent Yield Surface for Isotropic Hardening Material

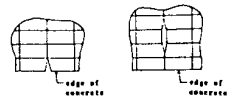

(a) Exterior crack (b) Interior crack

Fig. 8 Discrete Crack Model

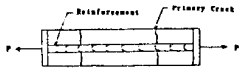

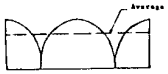

Stress in Concrete

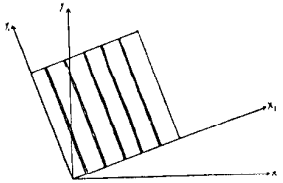

Fig. 9 Smeared Crack Model

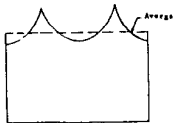

Stress in Reinforcement

Fig. 10 Stress Distribution in a Cracked Reinforced Concrete Element

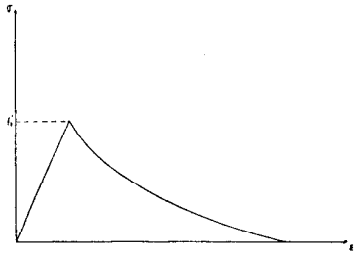

Fig. 11 Gradually Unloading Curve for Concrete (Lin and Scordelis, 1975)

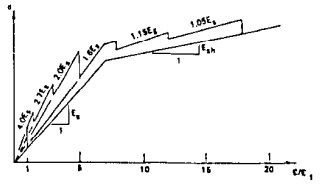

Fig. 12 Modified Stress-Strain Diagram for Reinforcing Steel (Gilbert and Warner, 1978)

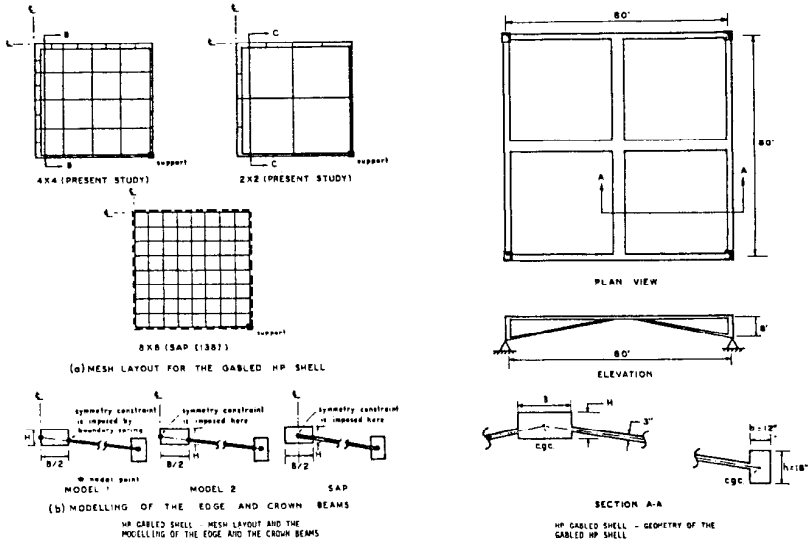

Fig. 13 HP Gabled Shell

(Chan, 1982)

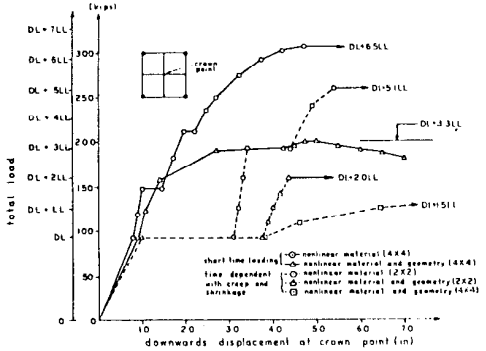

Fig. 14 Gabled HP Shell - Comparison of Load vs. Crown Point Vertical Downwards Displacement for Instantaneous and Sustained load (BxH = 48x12 in.)

(Chan, 1982)

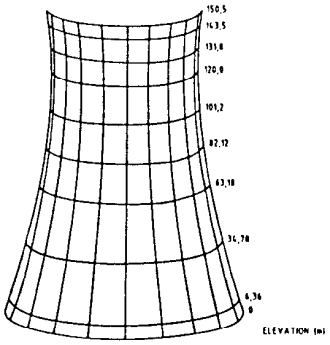

Fig. 15 Finite Element Mesh For Cooling Tower

(Milford and Schnobrich, 1984)

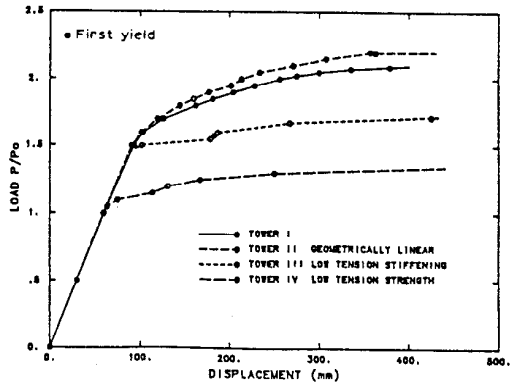

Fig. 16 Load-Displacement Curves for Windward Meridian

(Milford and Schnobrich, 1984)